geoconvention
Calgary • Canada • May 13-17 2019

Analytic models of distributed acoustic sensing data for straight and helical fibre

Heather K. Hardeman-Vooys, Michael P. Lamoureux
CREWES – University of Calgary, Department of Mathematics and Statistics

Summary

We discuss the process of acquiring seismic data using distributed acoustic sensing. We then describe the analytic model used to depict this process mathematically. We find the strain tensor for the full-waveform by separating the problem in to the case for the P-wave strain tensor and the S-wave strain tensor. We show examples of the model for the P-wave response of the fibre in two different media. We compare the results of the S-wave response for helical and straight fibre. Finally, we examine the full-waveform response of the fibre and consider the results using different gauge lengths.

Acquisition using DAS and Fibre Optic Cables

In seismic acquisition, a fibre optic cable is installed in a specific configuration. In this project, we consider a fibre optic cable buried horizontally 10 meters beneath the earth's surface over 100 m. A source is positioned in the centre of the fibre at the Earth's surface. Once the source detonates, it sends waves into the ground. When these waves hit the fibre, they stretch and strain the fibre optic cable. The strain on the fibre is recovered by an interrogator attached to the cable using a laser pulse that interacts with imperfections in the cable.

In the case of constant velocity, seismic waves move through the earth's subsurface in a spherical shape. In fact, an exercise in calculus shows that the Laplace operator can be considered in terms of radial solutions. We utilize the solution u of the acoustic wave equation written in terms of the P-wave and S-wave components

$$u = \nabla\Phi + \nabla \times \Psi$$

which can be derived from the wave equation using the Helmholtz Decomposition Theorem (Aki and Richards, 2002).

In this experiment, the strain is the measure of how much the wave moves the fibre. The equation for strain is defined as follows

$$\epsilon_{ij} = \frac{1}{2}\left(\partial_i u_j + \partial_j u_i\right).$$

The strain ϵ is a symmetric 3×3 matrix with three eigenvectors and three eigenvalues which describe how much the material moves in each of three orthogonal directions.

To recover the response of the fibre, we consider the fact that the wave hits the fibre at any given point $\mathbf{p}(\boldsymbol{s_0})$ where $\mathbf{p}$ is the path of the fibre. At some point in space, the fibre-optic cable has a tangent vector $\mathbf{T_p} = \mathbf{T_p}(x, y, z)$, which we assume is normalized. The amount of stretching at this point is given by the product of the strain matrix with the tangent vector. Thus, we can determine the strain at this point on $\mathbf{p}$ by the following equation

$$A(s,t) = \mathbf{T_p}(s)\epsilon(\sqrt{\mathbf{p}(s)})\mathbf{T_p}'(s)$$

where the matrix $\epsilon\left(\sqrt{\mathbf{p}(s)}\right)$ is the strain at the point s on the path $\mathbf{p}$ of the fibre which is a distance $r = \sqrt{\mathbf{p}(s)}$ away from the source at the origin.

Comparing the Effects of Gauge Length

We will now show the results of the effect that different gauge lengths have on the full-waveform response. We use the max P-wave and S-wave velocity found in saturated shales as given in (Bourbiè et al., 1987). We only consider the vector $A = [0,0,1]$ for the S-wave potential as it produced the sharpest image for both straight and helical fibre (Hardeman-Vooys et al., 2018). Over a distance of 100 m, we compare the following gauge lengths: 5 m, 10 m, 20 m and 25 m.

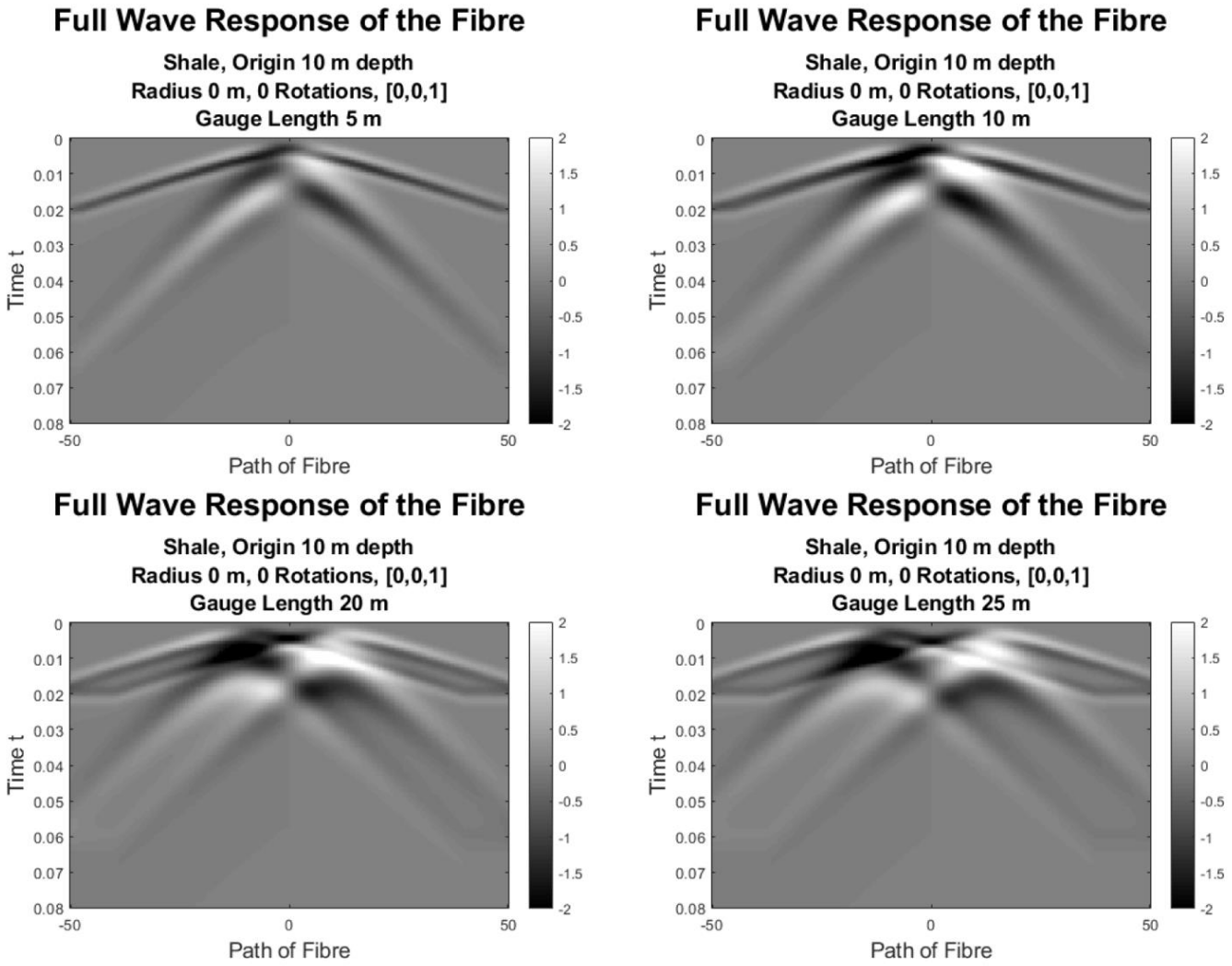

Figure 1: The full-wave response of the straight fibre in saturated shale when A = [0,0,1] for (top left) Gauge length 5 m, (top right) Gauge length 10 m, (bottom left) Gauge length 20 m, and (bottom right) Gauge length 25 m.

Fig. 1 shows the response of the straight fibre in shale for four different gauge lengths, where gauge length is a property of the DAS system related to the pulse width of the laser interferometer. The image is the sharpest for gauge length 5 m with the result for gauge length 10 m only slightly less sharp; however, we see a spreading of the hyperbola for gauge length 20 m and 25 m.

Recall that the gauge length considers the results of a small portion of the signal at a time, i.e. for our model: 5 m, 10 m, 20 m or 25 m. During that portion, gauge length is contracted or stretched depending on the shape of the signal. Since the response of the fibre is a hyperbolic, the larger gauge lengths contain a larger portion of the hyperbola. So, it holds more stretching and contracting information such

that the two could cancel each other out as seen in the spreading of the hyperbolas in the results for gauge length 20 m and 25 m.

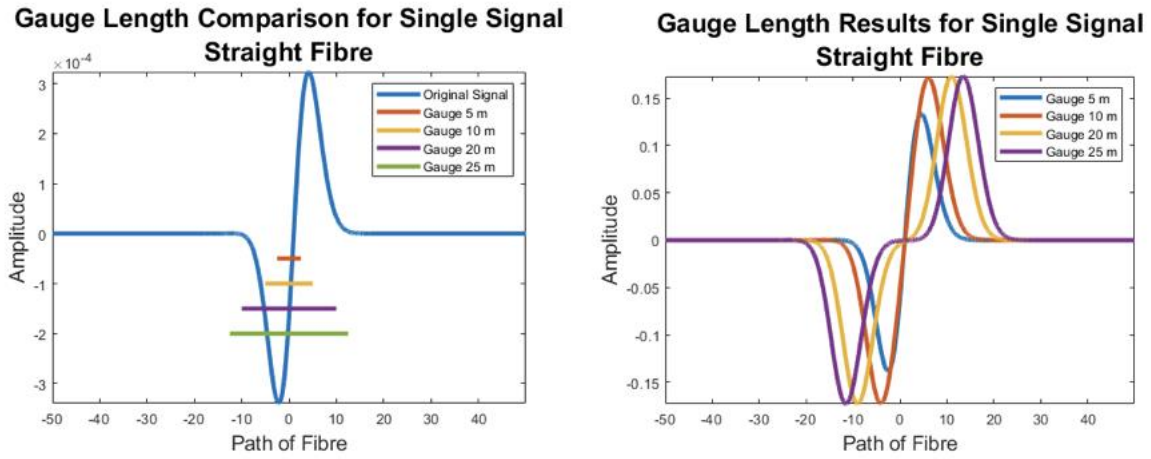

Figure 2: (Left) Comparison of the gauge lengths with respect to the full-waveform signal at t_1 of the straight fibre: (Blue) Original signal at t_1 (Red) Gauge length 5m, (Yellow) Gauge length 10m, (Purple) Gauge length 20m, and (Green) Gauge length 25m. (Right) Comparison of the gauge lengths applied to the full-waveform signal at t_1 of the straight fibre: (Blue) Gauge length 5m, (Red) Gauge length 10m, (Yellow) Gauge length 20m, and (Purple) Gauge length 25m.

Fig. 2 (left) gives a physical representation of what we described in the previous paragraph. The gauge length 5 m only contains an increasing portion of the signal around the origin. The gauge length 10 m contains some decreasing signal but mostly increasing signal around the origin. Both gauge length 20 m and 25 m contain a lot of increasing and decreasing portions of the signal enough to cancel out the response at the origin which we see occurs in Fig. 2 (right) for larger intervals around the origin as the gauge length increases. Fig. 2 (right) only describes what occurs for the first time step t_1 of the full-waveform response of the straight fibre. It provides a good visual explanation for the spreading which occurs for the larger gauge lengths in the bottom two images of Fig. 1.

While the helical fibre provides a dampened amplitude in comparison to the straight fibre, the helical fibre shows a similar spreading to the straight fibre between the different gauge lengths. As the gauge length gets larger, the signal spreads apart as it did with the straight fibre. Fig. 3 provides a reference of the first time step t_1 of the full-waveform response of the helical fibre to different gauge lengths. On the left, the gauge length has not been applied to the signal at the first time step t_1 of the full-waveform response of the helical fibre. On the right, the four different gauge lengths have been applied to the signal. As with the straight fibre, the larger gauge lengths contain more increasing and decreasing portions of the signal which cancel each other out resulting in the signal spreading. Also, the full-waveform response for the helical fibre results in a flattened peak for the hyperbolic response as the gauge length gets larger whereas the straight fibre's hyperbolic response resulted in multiple peaks.

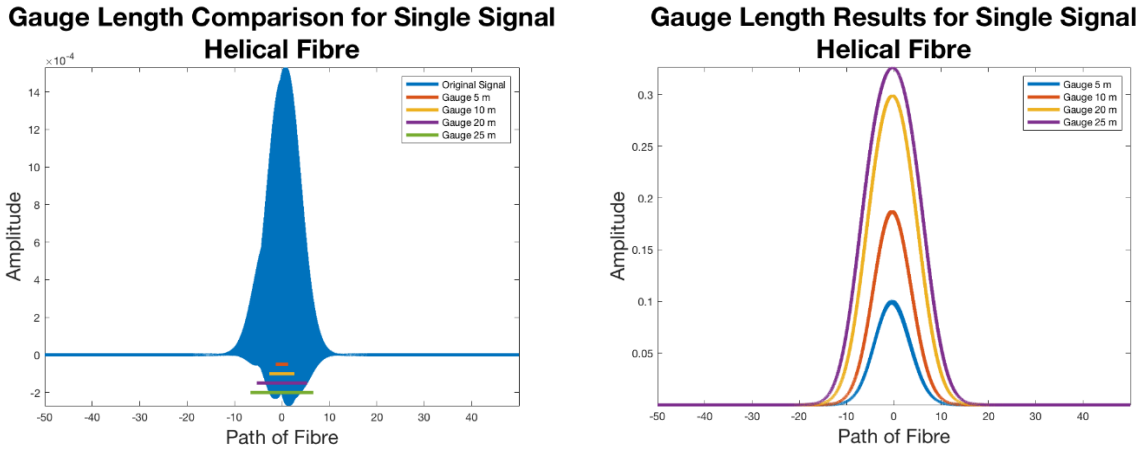

Figure 3:(Left) Comparison of the gauge lengths with respect to the full-waveform signal at t_1 of the helical fibre: (Blue) Original signal at t_1 (Red) Gauge length 5m, (Yellow) Gauge length 10m, (Purple) Gauge length 20m, and (Green) Gauge length 25m. (Right) Comparison of the gauge lengths applied to the full-waveform signal at t_1 of the straight fibre: (Blue) Gauge length 5m, (Red) Gauge length 10m, (Yellow) Gauge length 20m, and (Purple) Gauge length 25m.

Conclusions

We began with an explanation of the model. We studied the effects that different gauge lengths had on the full-waveform response for straight fibre. The larger gauge lengths produced a spreading in the response which was not found in the smaller gauge lengths. We noted that this is largely due to the amount of the signal contained in the larger gauge lengths which resulted in some cancellations.

Acknowledgements

We thank the sponsors of CREWES for their support. We also thank our colleagues at Fotech as well as CREWES for their support. We also gratefully acknowledge support from NSERC (Natural Science and Engineering Research Council of Canada) through the grants CRDPJ 461179-13, CRDPJ 522863 – 17, and through a Discovery Grant for the second author.

References

Aki, K., and Richards, P. G., 2002, Quantitative Seismology: University Science Books, Sausalito USA.

Bourbiè, T., Coussy, O., and Zinszner, B., 1987, Acoustics of porous media: Editions TECHNIP, Paris.

Hardeman-Vooys, H. K., and Lamoureux, M. P., 2018, Analytic models of distributed acoustic sensing data for straight and helical fibre: CREWES Research Report, 30, 1-17.